Fast crystallizing GeSb alloys for optical data storage

J. Solis, C. N. Afonso, J. F. Trull, and M. C. Morilla

Citation: J. Appl. Phys. **75**, 7788 (1994); doi: 10.1063/1.356584

View online: http://dx.doi.org/10.1063/1.356584

View Table of Contents: http://jap.aip.org/resource/1/JAPIAU/v75/i12

Published by the American Institute of Physics.

Fast crystallizing GeSb alloys for optical data storage

J. Solis, C. N. Afonso, J. F. Trull, and M. C. Morilla
Instituto de Optica, CSIC, C/Serrano 121, 28006 Madrid, Spain

(Received 1 November 1993; accepted for publication 9 February 1994)

A systematic study is presented on the optical and structural transformations induced in amorphous $Ge_{1-x}Sb_x$ alloys with Sb contents in the $0.71 \leq x \leq 0.91$ range by irradiation with 250 ns laser pulses. The results show that only those films richer in Sb than the eutectics ($x=0.85$) show appreciable optical contrast upon irradiation. The dominant role of Sb in the performances of this family of alloys is analyzed. The transition from a low-reflectivity amorphous phase to a high-reflectivity extended solid solution of Ge in crystalline Sb is shown to be the key for a new generation of fast reversible optical storage materials in which amorphous-crystalline cycling using ultrashort laser pulses is feasible.

I. INTRODUCTION

Phase-change optical storage takes advantage of the different optical properties that the amorphous and crystalline phases of a given material may present. Amorphization (writing process) can be easily accomplished by means of short laser pulses in order to induce melting and rapid solidification whereas crystallization (erasing process) usually requires longer laser pulses to induce both crystal nucleation and growth. One of the most important requirements for the full development of a phase-change-based technology is the availability of fast crystallizing media.[1] Fast crystallization and long-term stability of the amorphous phase are competing demands which need to be satisfied. To solve this problem the use of stoichiometric composition films[2] or materials with high glass temperature but still far from the melting temperature[3] has been proposed.

Several systems have been investigated aiming to decrease the minimum laser pulse length needed to induce crystallization to tens of nanoseconds. Most of them involve chalcogeneides and Sb alloys, i.e., GeTeSb,[4] InSbTe,[5] AgInSbTe,[6] GaSb,[7] or GeSb.[8] Systems in which crystallization can be triggered by pulses shorter than 100 ns (Refs. 7 and 8) have been nevertheless confined to write-once applications.[7] It has been recently demonstrated that they can be potential candidates for ultrafast subnanosecond reversible optical recording.[8]

GeSb is a simple eutectic system with a eutectic transformation at approximately 85 at. % Sb and 592 °C and at least one metastable GeSb phase.[9] Its phase diagram characteristics are similar to those of the GeTe system which is the most widely studied system for optical storage applications. The eutectics temperature of GeSb (and consequently the glass-forming temperature) is higher than that of GeTe system and therefore the stability of the amorphous phase can be enhanced. Furthermore, estimations of the time-temperature-transformation curves for pure Sb provide minimum transformation times shorter than 10 ns to achieve a crystallization fraction of 10^{-6}.[3] It is, therefore, expected that Sb-rich amorphous alloys will also be fast crystallizing materials. In fact, it has been recently shown that amorphous $Ge_{0.11}Sb_{0.89}$ and $Sb_{0.67}O_{0.33}$ thin films can be crystallized with picosecond laser pulses[10] and that reversible phase changes can be induced in $Ge_{0.10}Sb_{0.90}$ films by means of ultrashort laser pulses.[8] Nevertheless, to our knowledge no systematic studies of laser-induced phase changes in $Ge_{1-x}Sb_x$ films have been yet reported.

The present work aims to analyze laser-induced crystallization processes of $Ge_{1-x}Sb_x$ amorphous films with atomic composition x ranging from 0.91 to 0.71. The laser-induced crystallization upon irradiation with 250 ns laser pulses is analyzed by means of real-time reflectivity and transmission measurements which allow us to determine the transformation time and optical contrast. It is shown that those films with compositions x above 0.85 are fast crystallizing materials and the role of the Sb content in the crystallization kinetics is analyzed.

II. EXPERIMENT

Laser irradiation and real-time reflectivity measurements are performed using a two-laser-beam system. An acousto-optic pulsed Ar^+ laser (all lines) is focused on the sample to a $1/e$ beam radius of 4 μm for film irradiation. A He-Ne laser focused at the center of the former beam to a $1/e$ beam radius of 1.7 μm is used to follow in real time the evolution of the film reflectivity and transmission. The pulse length and power of the He-Ne laser is low enough to ensure that its thermal-induced effect is negligible.[11] A full description of the experimental setup can be found elsewhere.[12] For the present research we have selected a pulse length of 250 ns with energy densities in the 0–100 mJ/cm^2 range.

The samples are amorphous thin films grown in a multitarget dc magnetron sputtering from Ge and Sb targets (99.999%). The substrates (carbon-coated mica) are held at room temperature and placed in a rotating stage (2.7 rev s^{-1}) facing the targets. The system background pressure is 2.0×10^{-6} Torr and the operating Ar pressure is 4.0×10^{-3} Torr. The deposition rates are varied in the 0.2–0.3 nm s^{-1} range for germanium and the 0.7–2.2 nm s^{-1} for antimony in order to obtain the desired film composition. The film thickness is typically 50 nm.

Both as-grown and irradiated films are floated off the mica substrate in de-ionized water. Their structure and composition are then analyzed by transmission electron microscopy (TEM) and selected-area diffraction (SAD) in a JEOL

 0021-8979/94/75(12)/7788/7/$6.00

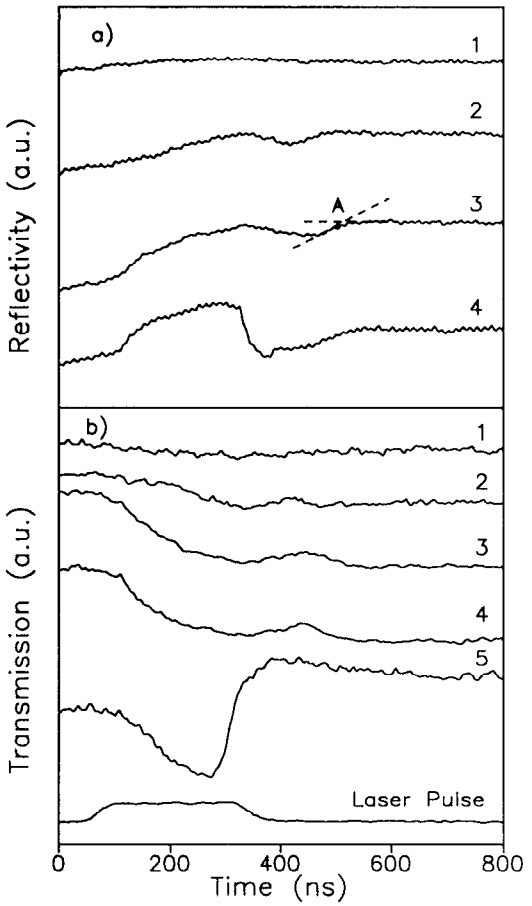

FIG. 1. (a) Real-time reflectivity and (b) transmission transients induced in $Ge_{0.09}Sb_{0.91}$ films upon irradiation with 250 ns laser pulses with energy densities of (1) 21, (2) 36, (3) 65, (4) 72, and (5) 94 mJ/cm^2. The dashed lines in transient 3(a) correspond to the solidification slope and the final reflectivity level. The cross between both lines, marked with A, corresponds to the time at which the material is fully solidified.

400 microscope equipped for energy-dispersive x-ray spectroscopy (EDX). The film compositions are determined within 5%. The surface morphology is studied by phase contrast reflection optical microscopy (PCROM).

III. RESULTS

The behavior of the films with Sb content richer than the eutectics (referred hereafter as Sb-rich compositions) upon irradiation is illustrated in Fig. 1. It shows several (a) real-time reflectivity (RTR) and (b) transmission (RTT) transients obtained upon irradiation of $x=0.91$ composition films. For the lowest studied energy densities the changes observed in reflectivity and transmission are close to the experimental resolution (Fig. 1, transients 1) and lead to a final reflectivity (transmission) level 2%–3% higher (lower) than the initial one. Higher-energy densities induce a reflectivity increase up to a maximum value followed by a dip (minimum) [transients 2,3 in Fig. 1(a)]. This minimum value occurs once the laser pulse has already ended and its temporal position as well as that of the maximum prior to the dip do not depend on the pulse energy density. Both the reflectivity value at the maximum and at the dip reach a saturation value as the energy density is increased. The behavior observed in transmission is symmetric [transients 2,3 in Fig. 1(b)]. In all cases, a high-reflectivity (low-transmission) material is produced after irradiation. At the highest energy densities, an abrupt decrease in the reflectivity transients with no equivalent in transmission [Fig. 1(a), transients 4], evidences the presence of topography effects.[11,13,14] This has also been confirmed by PCROM observations. If the energy density is further increased the transmission transients develop an abrupt increase [Fig. 1(b), transient 5] which corresponds to a hole opening process;[15] the reflectivity transients being similar to transient 4 in Fig. 1(a). Since both topography and hole opening processes usually occur via liquid-phase formation, the appearance of the abrupt reflectivity decrease or transmission increase in the transients indicates that the pulse energy density used is above the melting threshold. The general features in RTR and RTT transients described for this composition film are common to the films with Sb content higher than $x=0.85$, the topography and hole opening thresholds, and the optical contrast upon irradiation being a function of the Sb content.

The characteristic morphologies obtained upon irradiation are shown in Fig. 2 for the $x=0.91$ composition film. At low energy densities [Fig. 2(a)] the irradiated region shows the presence of asymmetrically distributed crystalline material. The crystalline morphologies are circular islands showing extinction contours and exhibiting a radial growth commonly observed in solid-state annealing processes. Since the size of these crystalline areas is smaller than the diameter of the probe beam, the corresponding RTR transient (transient 1 in Fig. 1) accounts from both transformed and untransformed regions.[16] It is then nearly featureless and evidences the presence of crystalline regions as a slight ($\approx$2%) contrast change. At a higher energy density a larger single circular crystalline area is observed showing laminar crystals with characteristic extinction bands like those typically observed under melting/rapid solidification[8] [Fig. 2(b), exhibiting transients like 2 and 3 in Fig. 1]. Morphologies intermediate between the ones shown in Figs. 2(a) and 2(b) are also observed upon irradiation with low and intermediate energy densities [Fig. 2(c)]. The micrograph shows crystalline regions formed by the addition of different crystalline islands where the two morphologies described above, i.e., radial crystals and laminar crystals with extinction bands, can both be seen. The SAD patterns of the crystalline regions, also included in the figure, show in all cases the presence of crystalline Sb with no clear evidence of other crystalline phases.

In the films with Sb content below the eutectics (referred hereafter as Ge-rich compositions), the transient reflectivity changes induced are very weak (in the order of 1%–2% maximum transient reflectivity increase) and no appreciable permanent reflectivity changes are observed for fluences below the topography threshold. The transmission transients, however, present two different regimes as the pulse energy density increases as can be seen in Fig. 3 for the $x=0.74$ composition films. At low energy densities, the transmission transients show a smooth decrease followed by an increase to a final level slightly lower than the initial one (transient 1 in Fig. 3). The minimum transient transmission value occurs at

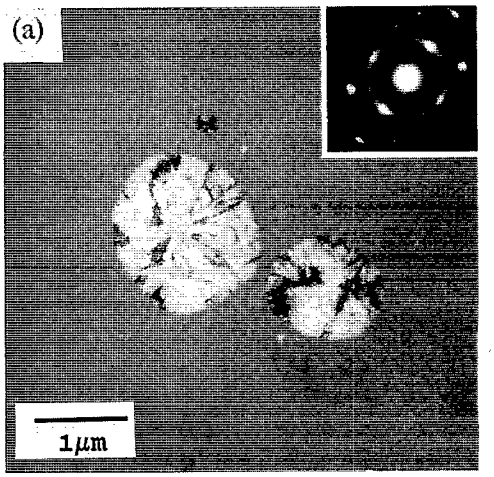

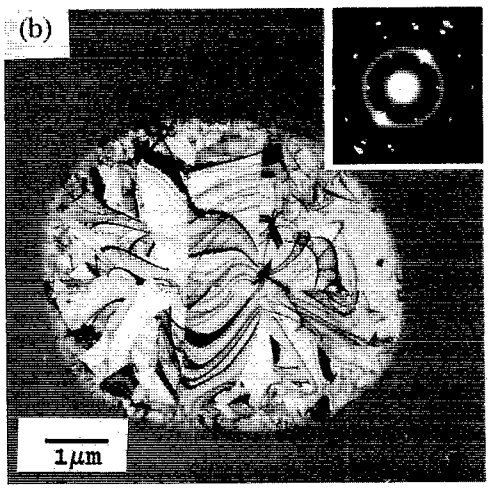

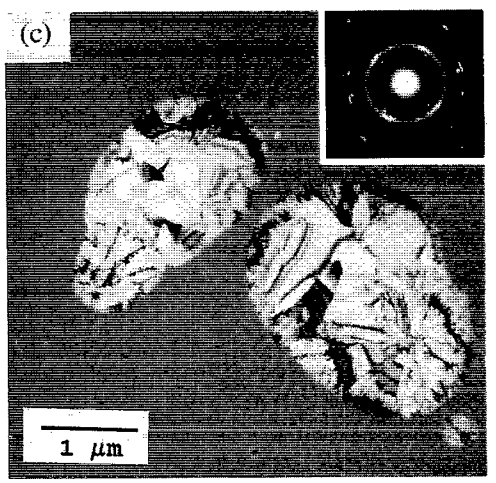

FIG. 2. TEM micrographs corresponding to $Ge_{0.09}Sb_{0.91}$ films upon irradiation with 250 ns laser pulses with (a), (c) 21 and (b) 58 mJ/cm^2. The SAD patterns of the crystalline regions are also included.

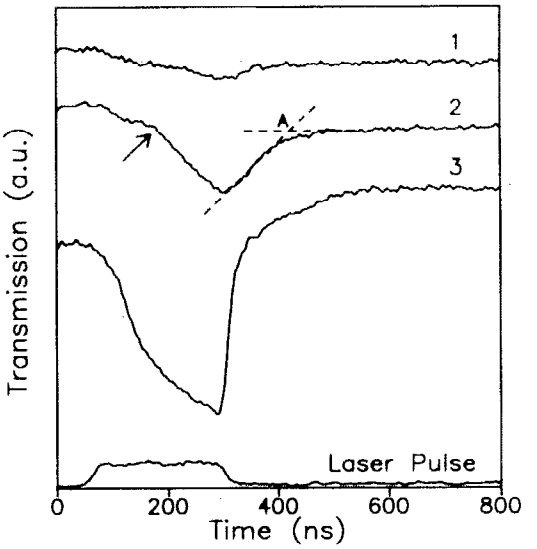

FIG. 3. Real-time transmission transients induced in $Ge_{0.29}Sb_{0.71}$ films upon irradiation with 250 ns laser pulses with energy densities of (1) 36, (2) 51, and (3) 94 mJ/cm^2. The arrow points out characteristic slope change associated to the melt onset. The dashed lines in transient 2 correspond to the solidification slope and the final transmission level. The cross between both lines, marked with A, corresponds to the time at which the material is fully solidified.

the pulse end. When the energy density is higher the transmission decreases but a clear slope change is now observed in the decreasing part of the transmission transients. Transmission again reaches a minimum value with the pulse end, to increase then to a value always lower than the initial one (transient 2 in Fig. 3). The transmission intensity at which the slope change occurs is constant for a given composition. Topography effects can be observed by PCROM only for fluences in which the slope change is present in the transients. The fact that the transmission intensity at the inflection is constant[13] and that topography effects usually occur via liquid-phase formation allows us to correlate the slope change in the transmission transients with the presence of melting. The minimum observed for fluences below the hole opening threshold is then related to the liquid-phase cooling onset. For the highest energy densities the transmission recovery after the minimum occurs abruptly before the pulse end and the final level is higher than the initial one evidencing that a hole opening process has taken place (transient 3 in Fig. 3). The irradiated regions present typically amorphous phases except for the $x=0.79$ composition films in which some evidence of crystalline phases is observed.

The optical contrast induced upon irradiation both in reflectivity and in transmission as a function of the pulse energy density is shown in Fig. 4. R_f, R_i, T_f, and T_i denote the final f and initial i reflectivity R and transmission T values, respectively. The vertical axis in Fig. 4 has been defined in order to plot both R and T contrast values in a positive scale. For a given composition film, the optical contrast in reflectivity and transmission is an increasing function of the pulse energy density until the thresholds for topography effects and hole opening are reached, respectively, as confirmed by optical microscopy observations. Since the lateral and depth extension of the transformed region increase as the energy density increases, the optical contrast is expected to be an increasing function of the energy density

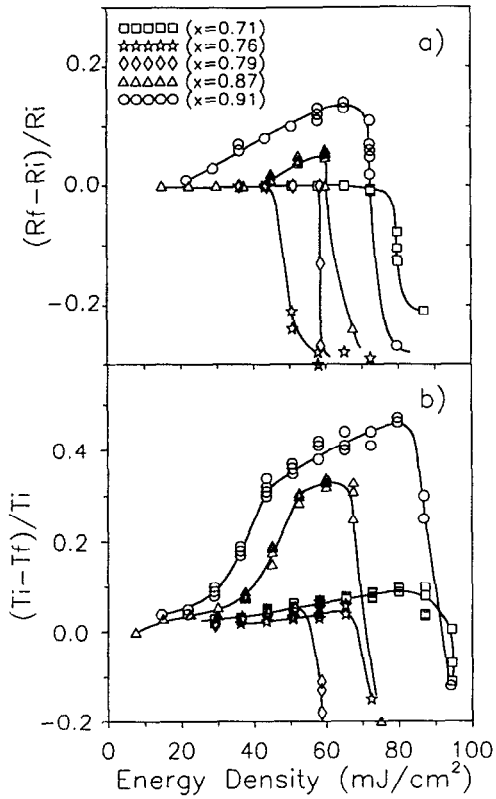

FIG. 4. Optical contrast in reflectivity $[(R_f-R_i)/R_i]$ and transmission $[(T_i-T_f)/T_i]$ induced upon irradiation vs laser pulse energy density for films with different Sb content x. R_f, R_i, T_f, and T_i correspond to the reflectivity R and transmission T values before i and after f irradiation.

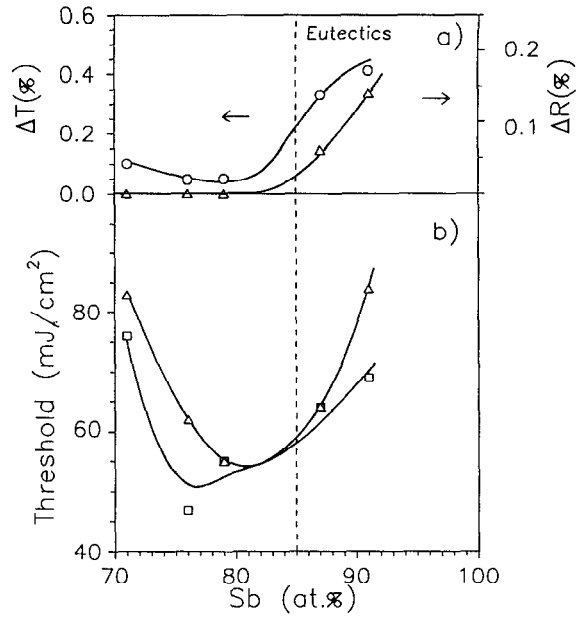

FIG. 5. Maximum optical contrast in (a) reflectivity (ΔR,△) and transmission (ΔT,○), and (b) topography (□) and hole opening thresholds (△) upon irradiation vs film composition. The solid lines are a guide to the eye and the dashed vertical line corresponds to the eutectics composition.

until the size of the transformed area is larger than the probe beam diameter[16] as observed experimentally. The topography and hole opening thresholds are evidenced by the sudden decrease followed by change in the sign of the optical contrast in reflectivity and transmission, respectively.

The maximum optical contrast in R and T, together with the topography effect and hole opening thresholds, are plotted in Fig. 5 as a function of the composition. The dashed vertical line corresponds to the eutectics. The Sb-rich films ($x>0.85$) present strong optical contrast upon irradiation both in R and T which is an increasing function of the Sb content. The Ge-rich films exhibit instead a nearly negligible contrast. The two thresholds plotted in Fig. 5(b) curves present an inflection in the neighborhood of the eutectics.

IV. DISCUSSION

The RTR and RTT transients obtained in the Sb-rich films show clearly that the transformation kinetics in these films is very different to the one observed in the Ge-rich films. The RTR transients obtained in the former films at intermediate fluences show a characteristic dip with a reflectivity level which is ≈6% below the final one. The reflectivity of Sb at the probe beam wavelength is 0.71 whereas that of the liquid material is 0.67 (6% lower). Since crystalline Sb is the only phase observed upon irradiation, the reflectivity increase after the dip can be consistent with solidification and cooling of crystalline Sb. In order to support this interpretation we have simulated the reflectivity of a $Ge_{0.09}Sb_{0.91}$ film as it melts or solid state crystallizes, assuming that the optical properties of the liquid and the crystalline material are similar to those of pure Sb. The reflectivity of a $Sb/Ge_{0.09}Sb_{0.91}$/substrate system is simulated as a function of the Sb layer thickness, the sum of the thickness of the Sb and GeSb layers being constant and equal to the total film thickness. The Sb surface layer is either liquid (l-Sb) or polycrystalline (p-Sb) and the innermost layer is amorphous $Ge_{0.09}Sb_{0.91}$. The optical constants used in the simulation are $n=2.87$, $k=4.5$ for l-Sb,[17] $n=2.85$, $k=5.03$ for p-Sb,[18] and $n=3.47$, $k=3.17$ for amorphous $Ge_{0.09}Sb_{0.91}$.[19] The results are shown in Fig. 6 where it can be clearly seen that the reflectivity of the system with a liquid layer at the surface is always lower than the equivalent system with a p-Sb layer at the surface. The characteristic shape of a RTR transient obtained in the Sb-rich films has also been included in Fig. 6 in order to facilitate the comparison of the simulation and experimental results. This curve has to be considered as an intuitive representation since it is not straightforward to plot both data in the same horizontal scale. In addition, the reflectivity changes experimentally measured may depend on the extension of the transformed region.[14] Upon irradiation, the reflectivity first increases, reaches a maximum value and then decreases. Since a transition from a polycrystalline solid material to a liquid one should necessarily involve a decrease in the reflectivity, the initial reflectivity increase in the RTR transient is most likely related to a solid-phase crystallization process and the reflectivity maximum prior to the dip should correspond to the melt onset. At some time after the irradiation pulse end the experimentally observed reflectivity reaches a minimum value which is consistent with the formation of a liquid layer at the surface. Since the reflectivity

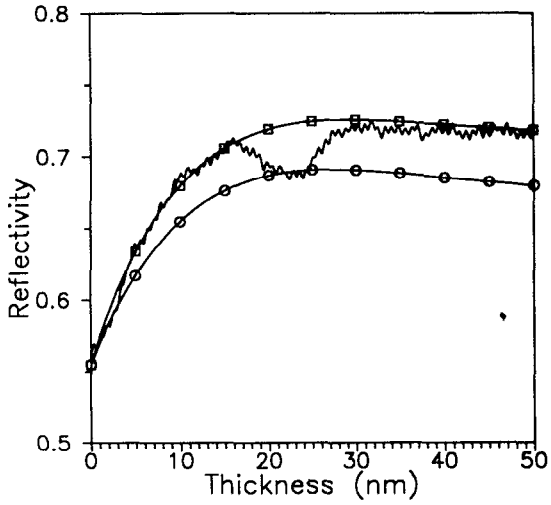

FIG. 6. Reflectivity of a $Sb/Ge_{0.09}Sb_{0.91}$/substrate multilayer system as a function of the thickness of the surface layer, the sum of the thicknesses of the Sb and GeSb layers being constant and equal to 50 nm. The Sb surface layer is either liquid (l-Sb) (○) or polycrystalline (p-Sb) (□) and the inner layer is amorphous $Ge_{0.09}Sb_{0.91}$. The characteristic shape of a RTR transient obtained in the Sb-rich films has been also included.

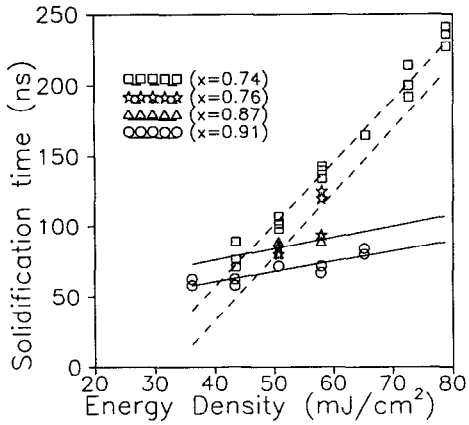

FIG. 7. Solidification time vs pulse energy density for the different studied film compositions. The solid and dashed lines are linear fits of the data corresponding to the Ge-rich (dashed line) and the Sb-rich (solid line) compositions.

at the minimum does not remain at this value a significant amount of time, the melt depth induced should not be much deeper than the thickness above which the probe beam "sees" a bulk liquid. Finally, the experimental reflectivity curve increases to reach a value which corresponds to the crystalline state, this increase being therefore related to the liquid-phase cooling and solidification processes. Since the optical properties of the liquid do not depend significantly on temperature,[17] the reflectivity increase after the minimum is mainly caused by the decrease of the liquid layer thickness. It is, therefore, a reasonable approximation to consider that the solidification onset occurs at the time the reflectivity reaches the minimum.

The former interpretation of the RTR transients is also in agreement with the characteristics of the induced microstructures. At low energy densities, the RTR transients show no dip and the irradiated areas show the existence of crystallized material [see Fig. 2(a)]. The crystals exhibit a radial growth similar to that typically observed in solid-phase annealing processes. When the energy density is increased and the dip is observed in the transients, the morphology of the crystals produced in the irradiated area is similar to that typically observed upon a melting-rapid solidification process.[8] From the analysis of the RTR transients we can also see that melting is always preceded by crystallization in the Sb-rich films and occurs preferentially in the previously crystallized zones as evidenced in Fig. 2(c). A picture of the induced process can be seen as follows. When the laser fluence is enough to activate the crystallization process, the film crystallizes producing most probably Sb crystals with a high density of defects due to the high thermal gradients involved. The melting temperature of these crystals is then lower than that of bulk Sb,[20,21] and the heat released upon crystallization is enough to increase the temperature further to the melting point.

Melting is evidenced in the reflectivity transient of the Sb-rich composition films by the presence of a dip (minimum) whose temporal position provides the solidification onset. The cross between the linear extrapolation of reflectivity increase after the minimum (solidification process) and the final reflectivity level provides the instant at which the material is fully solidified (see Fig. 1 transient 3). The temporal interval between these two times (solidification onset and end) provides the solidification time. In the case of the Ge-rich films, melting is evidenced by a slope change in the decreasing part of the transmission transients and the solidification time can be obtained similarly from the minimum in the transmission transient, which corresponds again to a good approximation to the solidification onset, and the final transmission level (see Fig. 3, transient 2).

The solidification times for the different studied composition films versus the laser fluence are shown in Fig. 7. For each composition the leftmost point corresponds to a value just above the melting threshold whereas the right-handmost one corresponds to a fluence just below the hole opening threshold. The proximity between both thresholds for $x=0.79$ composition films does not allow us to plot the data corresponding to these films. Figure 7 shows that the Sb-rich films solidify much faster than the Ge-rich ones, and that the solidification time always follows a similar linear behavior but with two very different slopes: ≈ 4.4 ns $(\text{mJ})^{-1}\,\text{cm}^2$ for the Ge-rich films and 0.76 ns $(\text{mJ})^{-1}\,\text{cm}^2$ for the Sb-rich ones. It is also worth noticing that the extrapolation to zero energy in the Sb-rich films yields an apparent solidification time for zero laser fluence. Figure 7 provides additional information which is worth discussing. In a general situation of a liquid layer on top of a substrate it is clear that the solidification time should increase with the temperature of the liquid, the cooling rate being controlled by the conductivity of the liquid and the substrate. The fact that both the Ge-rich and the Sb-rich films show the same linear behavior with a strong slope jump at the eutectics might suggest that the thermal conductivity of the liquid would be discontinuous at the eutectics composition. However, since the thermal con-

ductivity of the liquid is expected to be a second-order effect, a more plausible explanation could be the presence of two very different melting/solidification scenarios for both composition regimes. The faster solidification times observed in the Sb-rich films could be related to the presence of a solidification phenomena occurring through bulk nucleation[22] in a highly supercooled liquid[23] as reported in the case of GeTe alloys[24] and amorphous Si upon[25] irradiation with ns laser pulses. The absence of Ge segregation upon solidification in the Sb-rich films clearly indicates that solidification has occurred far below [at least 100–200 K (Ref. 9)] the thermodynamic melting temperature which supports this hypothesis.

The results plotted in Fig. 5 show that the separation between the Ge-rich and the Sb-rich behaviors occurs around the eutectics ($x=0.85$) although it can be shifted to a lower value. According to a tentative metastable phase diagram of the GeSb system[9] obtained from splat quenching experiments, the composition $x=0.83$ is the proposed limit for the development of solid solutions of Ge in Sb with no presence of other stable or metastable phases and with a very small change in the lattice parameters of pure Sb. Laser-mixing experiments of Ge/Sb multilayers have also shown that crystalline Sb can incorporate up to $\approx$20% Ge dissolved in its lattice with no significant variation of the lattice spacing of Sb.[26] These facts give us further basis to conclude that the optical contrast in reflectivity upon crystallization of the films with Sb content above the eutectics is due to a transition in which the final state is a semimetallic high-reflectivity phase showing a behavior basically similar to that of Sb but with a reflectivity which increases with the Sb content as seen in Fig. 5(a). It is therefore clear that the Sb content plays the dominant role for inducing at the same time strong optical contrast and fast crystallization times. The Ge content in the Sb-rich films is merely an agent which reduces the mobility of the Sb atoms and provides enough stability to the amorphous phase. A similar role for the Sb has been previously observed in laser-induced crystallization of Sb-rich films in Sb_xO_{1-x} and $In_{1-x}Sb_x$ films.[10,27] This conclusion is further confirmed by the results provided in Ref. 8 in which the reversibility of the crystallization process in GeSb films with composition $x=0.91$ by irradiation with pico- and femtosecond laser pulses was demonstrated. In that work the crystalline material was obtained under ns laser pulse irradiation through melting with no segregation of Ge. Subsequent irradiation with ps/fs laser pulses induced the formation of an amorphous phase with similar optical properties to the as-deposited material. Therefore, both crystallization and amorphization have to occur through a process in which the Ge and Sb atoms in the liquid phase are "quenched" in their positions through a diffusionless process.

A new generation of fast reversible phase-change optical recording materials based on structural transitions between nonstoichiometric low-reflectivity amorphous films and high-reflectivity extended solid solutions can be foreseen from the present results. It has been shown that this new generation of materials can be cycled between the amorphous and the crystalline states using ps and fs pulses.[8] This is in contrast with previously proposed materials in which the use of stoichiometric or nearly stoichiometric alloys and partitionless crystallization mechanisms were pointed out to be a necessary requirement[28] for fast crystallization and reversibility. The fact that crystallization is reached through melting in the Sb-rich composition film does not affect our main conclusion since it has been recently demonstrated that melt-erasing mechanisms[29,30] improve the erase performances and provide wider erase power margins.

V. CONCLUSIONS

Our results show that only those composition films with Sb content $x>\approx 0.85$ (Sb rich) show appreciable optical contrast in reflectivity upon crystallization, the crystallization times being much shorter than in $x<0.85$ composition films (Ge rich). The solidification speed is higher for the Sb-rich than for the Ge-rich films and the former are found to solidify in a crystalline phase in times of the order of tens of ns. High contrast and short-pulse-induced crystallization in the Sb-rich films can, therefore, be simultaneously achieved. Sb plays a major role in inducing those characteristics since crystallization occurs through a transition between a low-reflectivity amorphous phase and a high-reflectivity crystalline extended solid solution of Ge in Sb which shows a behavior similar to that of Sb. A new generation of materials for fast reversible optical storage can then be foreseen from these results.

ACKNOWLEDGMENTS

This work was partially supported by the Comisión Interministerial de Ciencia y Tecnología (CICYT, Spain) under Program TIC93. We greatly acknowledge Dr. F. Catalina (I. de Optica del CSIC, Madrid) and M. A. Ollacarizqueta (CIB, CSIC, Madrid) for many fruitful discussions and Y. Garcia (I. de Optica, CSIC, Madrid) for technical assistance.

[1] K. A. Rubin, Mater. Res. Soc. Symp. Proc. **230**, 239 (1992).
[2] M. Chen, K. A. Rubin, and R. Barton, Appl. Phys. Lett. **49**, 1255 (1986).
[3] F. Jiang and M. Okuda, Jpn. J. Appl. Phys. **30**, 97 (1991).
[4] M. Suzuki, K. Furuya, K. Nishimura, A. Andoh, N. Tsuboi, and M. Nagi, Proc. SPIE **1316**, 267 (1990).
[5] Y. Maeda, H. Andoh, I. Ikuta, and H. Minemura, J. Appl. Phys. **64**, 1715 (1988).
[6] H. Iwasaki, Y. Ide, M. Harigaya, Y. Kageyama, and I. Fujimara, Jpn. J. Appl. Phys. **31**, 461 (1992).
[7] D. J. Gravesteijn, H. M. van Tongeren, M. Sens, T. Bertens, and C. J. van der Poel, Appl. Opt. **27**, 736 (1988).
[8] C. N. Afonso, J. Solis, F. Catalina, and C. Kalpouzos, Appl. Phys. Lett. **60**, 3123 (1992).
[9] B. C. Giessen and C. Borromee-Gautier, J. Solid State Chem. **4**, 447 (1972).
[10] C. N. Afonso, M. C. Morilla, J. Solis, N. H. Rizvi, M. A. Ollacarizqueta, and F. Catalina, Mater. Sci. Eng. A **173**, 343 (1993).
[11] J. Solis, C. Ortiz, C. N. Afonso, and F. Catalina, Appl. Phys. A **54**, 279 (1992).
[12] J. Solis and C. N. Afonso, J. Appl. Phys. **69**, 2105 (1991).
[13] J. Solis and C. N. Afonso, J. Appl. Phys. **72**, 2125 (1992).
[14] C. N. Afonso, J. Solis, and F. Catalina, Mater. Sci. Eng. B **7**, 169 (1990).
[15] M. Chen, V. Marello, and U. G. Gerber, Appl. Phys. Lett. **41**, 894 (1982).
[16] C. N. Afonso, J. Solis, and F. Catalina, Appl. Surf. Sci. **43**, 171 (1989).
[17] R. Serna, J. Solis, and C. N. Afonso, J. Appl. Phys. **73**, 3099 (1993).
[18] J. C. G. de Sande, F. Vega, C. N. Afonso, C. Ortega, and J. Siejka (unpublished).

[19] J. C. G. de Sande (optical constants determined by spectroscopic ellipsometry, private communication).
[20] D. Wolf and S. Yip, Mater. Res. Soc. Symp. Proc. **230**, 3 (1992).
[21] D. Turnbull, Contemp. Phys. **10**, 473 (1969).
[22] S. R. Stiffler, M. O. Thompson, and P. S. Peercy, Phys. Rev. Lett. **60**, 2519 (1988).
[23] In this article we use undercooling to refer to the deviation of an interface from the melting temperature and supercooling to refer to the deviation of a bulk liquid from the melting temperature.
[24] Y. Nakayoshi, Y. Kanemitsu, and Y. Matsumoto, Jpn. J. Appl. Phys. **31**, 71 (1992).
[25] J. S. Im, H. J. Kim, and M. O. Thompson, Appl. Phys. Lett. **63**, 1969 (1993).
[26] R. Serna, C. N. Afosno, A. K. Petford-Long, and N. J. Long, Appl. Phys. A **56**, 132 (1993).
[27] J. Solis, K. A. Rubin, and C. Ortiz, J. Mater. Res. **5**, 190 (1990).
[28] K. A. Rubin and M. Chen, Thin Solid Films **181**, 129 (1989).
[29] Y. Maeda, I. Ikuta, H. Ando, and Y. Sato, Jpn. J. Appl. Phys. **31**, 451 (1992).
[30] T. Iijima, T. Tanabe, and N. Fukuyoshi, Jpn. J. Appl. Phys. **28**, L1985 (1989).